CRITICAL REVIEW: TREATMENT METHODS FOR SHORT-CHAIN PFAS

Sumedh Kothari

0. ABSTRACT

With global industries switching from long-chain per- and poly- fluoroalkyl substances (PFAS) to short-chain PFAS (C=4-7), short-chain PFAS are becoming a growing health concern. Short-chain PFAS have been detected in water throughout the world at concentrations exceedingly above regulatory standards, yet the majority of studies focus on the removal of long-chain PFAS. The main objective of this review is to provide a critical analysis on novel techniques for short-chain PFAS removal from water. The study looks at adsorption and membrane separation as the two primary treatment methods as well as the effects of external factors such as organic matter, pH, and ionic concentration. Overall, membranes such as nanofiltration and reverse osmosis that incorporated an adsorbent component performed the best when removing short-chain PFAS. However, further research needs to be completed on many removal techniques when it comes to testing real feedwater with additional contamination, such as the presence of organic matter.

1. INTRODUCTION

Per- and poly-fluoroalkyl substances (PFAS) are surfactants used in industrial applications and frequently found in everyday products, including nonstick pans, stain-resistant fabrics, and fire retardants. Although their properties make them useful across a variety of industries, PFAS molecules do not biodegrade quickly and are known as “forever chemicals.” PFAS chemicals have been found in low concentrations in many bodies of water, including rivers, lakes, groundwater, drinking water, and marine waters (Rayne and Forest, 2009). Humans are widely exposed to PFAS chemicals through drinking water, and PFAS has been detected in blood samples (Daly et al., 2018). PFAS chemicals have been linked with causing immunotoxicity, thyroid disease, liver disease and cancer, lipid and insulin dysregulation, kidney disease, uric acid, kidney cancer, and adverse reproductive outcomes (Fenton et al., 2021). Due to the bioaccumulation ability of these forever chemicals, the continued exposure increases the risk for everyone.

Due to the strength of the carbon-fluorine bond, PFAS have desirable properties for use in industrial and consumer products. For example, PFAS are hydrophobic and oleophobic by nature due to their perfluorocarbon moieties. They also can lower the surface tension of water significantly, and this can be seen in their use in chrome plating, where PFAS are used to prevent the evaporation of hexavalent chromium [Cr(VI)] vapor due to the lower surface tension of the electrolyte solution (Glüge et al., 2020). As a result, PFAS are widely used in various industries, including electronics, energy, textiles, food packaging, and pharmaceuticals (Glüge et al., 2020).

The first regulation for PFAS was the 2004 Stockholm Convention on Persistent Organic Pollutants. It laid the framework for global PFAS regulation (OECD 2023), labeling them as Persistent Organic Pollutants (POPs) and ultimately resulting in trade restrictions for PFOS and PFOA as well as national release action plans for those chemicals. Other regulations include the Toxic Substances Control Act and the most recent Environmental Protection Agency (EPA) PFAS National Primary Drinking Water Regulation. The Toxic Substances Control Act required companies to report their use of long-chain perfluoroalkyl carboxylate chemicals (LCPFAC) to the EPA within 90 days (US EPA, 2015), aiming to formalize voluntary industry commitment to phase out

LCPFAC by the end of 2015 (US EPA, 2015). Recently, there was a landmark court case where 3M, one of the companies that produces PFAS chemicals, offered $10 billion to settle claims of PFAS contamination in 12,000 water systems in the US and to help water treatment facilities recoup the costs of removing these chemicals (Bloomberg Law, 2024). Due to growing evidence of the negative health impacts of these chemicals, the EPA established new PFAS regulations in 2024, placing a maximum concentration level of PFOS and PFOA at 4 ppt (parts per trillion) in drinking water (EPA 2024). To avoid these strict regulations, many industrial companies have switched to using short-chain PFAS in their products, which have similar properties but are known to break down more quickly than long-chain PFAS (Danish Environmental Protection Agency, 2015). Since short-chain PFAS have higher mobility in water than long-chain compounds as they are more easily dissolved than long-chain PFAS (Gagliano et al., 2020), they could specifically affect and contaminate drinking water. More recently, short-chain PFAS have been detected frequently in surface water, perhaps due to the switch from long-chain to short-chain PFAS in industry (Bai and Son, 2021). Additionally, much of the literature has been based on the long-chain PFOA and PFOS molecules, and many of the proposed solutions for those long-chain removals need higher efficiencies for short-chain PFAS removal (Gagliano et al., 2020).

This review is a critical analysis of the limited research on the removal of short-chain PFAS from water to address the growing need caused by the transition of industry to the short-polyfluorinated chemicals. We examine the important properties of PFAS chemicals, focusing on short-chain compounds. By comparing the efficacy of different methods and materials for removing short-chain PFAS from water, this review will provide a direction for future water treatment research to address newly released “forever chemicals.” Lastly, we investigate the effects of the presence of organic matter, background ions, and pH on the removal of short-chain PFAS, to guide future treatment of a variety of water sources to meet strict regulations.

2. PFAS MOLECULES

2.1 PROPERTIES OF DIFFERENT PFAS MOLECULES

PFAS molecules have a variety of unique chemical properties, mainly stemming from their powerful C-F covalent bond, polar functional group head, and hydrophobic fluorocarbon chain. Due to the high electronegativity, high ionization potential, and low polarizability of fluorine, the C-F single bond is one of organic compounds’ strongest and most inert bonds. The bond, in particular, gives PFAS enormous thermal, physical, and chemical stability (see Table 1), allowing it to remain in the environment for a long time, hence their “forever chemical” title. Two common functional group heads are carboxylate (CO_2^-) and sulfonate (SO_3^-), which are polar and thus hydrophilic. The presence of a hydrophobic fluorocarbon chain and a hydrophilic head group makes PFAS an amphiphilic molecule (Alves et al., 2020), resulting in powerful surfactant properties (Leung et al., 2023). PFAS molecules can reduce the surface tension of water from 72 dyn/cm to 15-20 dyn/cm compared to only 25-30 dyn/cm for other hydrocarbons (Kirsch, 2013).

Table 1. Fluorine Characteristics and Effect on PFAS Properties (ITRC 2023)

Fluorine Characteristic	Description	Effect	Resulting Property of PFAS
High Electronegativity	Tendency to attract shared electrons in a bond	Strong C-F Bond	Thermal stability
			Chemical stability (low reactivity)
		Polar bond with partial negative charge toward F	Strong acidity (low pKa) [1]
Low polarizability	Electron cloud density not easily impacted by the electric fields of other molecules	Weak intermolecular interactions	Hydrophobic and lipophobic surfactant properties [2]
		Low surface energy	
Small size [3]	Atomic radius of covalently bonded fluorine is 0.72 A [4]	Shields Carbon	Chemical stability (low reactivity)

[1] Strong acidity when paired with an acid functional group such as carboxylic or sulfonic acid
[2] Hydrophobic and lipophobic surfactant properties when paired with a functional group that is hydrophilic (e.g., carboxylate)
[3] Small size due to having the smallest of the halogen atoms (fluorine)
[4] A = angstrom

However, due to the hydrophobic nature of the fluorocarbon chain, chain length affects the properties of PFAS molecules. Long-chain PFAS are more hydrophobic than short-chain PFAS because of the increased number of hydrophobic CF_2 groups (Ahrens and Bundschuh, 2014). As the carbon chain length increases, PFAS molecules become more inert, making them less likely to degrade. Additionally, their water solubility increases as their carbon chain length decreases due to the decreased hydrophobic nature of having a shorter hydrophobic fluorocarbon chain (Kucharzyk et al., 2017). Increasing chain length results in a more lipophilic molecule due to the increased hydrophobicity (see Figure 1). PFCAs and PFSAs have low vapor pressures, and as carbon chain length increases, the vapor pressure further decreases (Rahman et al., 2014). Due to the difference in these properties due to carbon chain length, techniques for the removal of long-chain PFAS molecules often do not work as efficiently for the removal of short-chain PFAS molecules, which is why finding novel techniques for the removal of these shorter PFAS chemicals is essential.

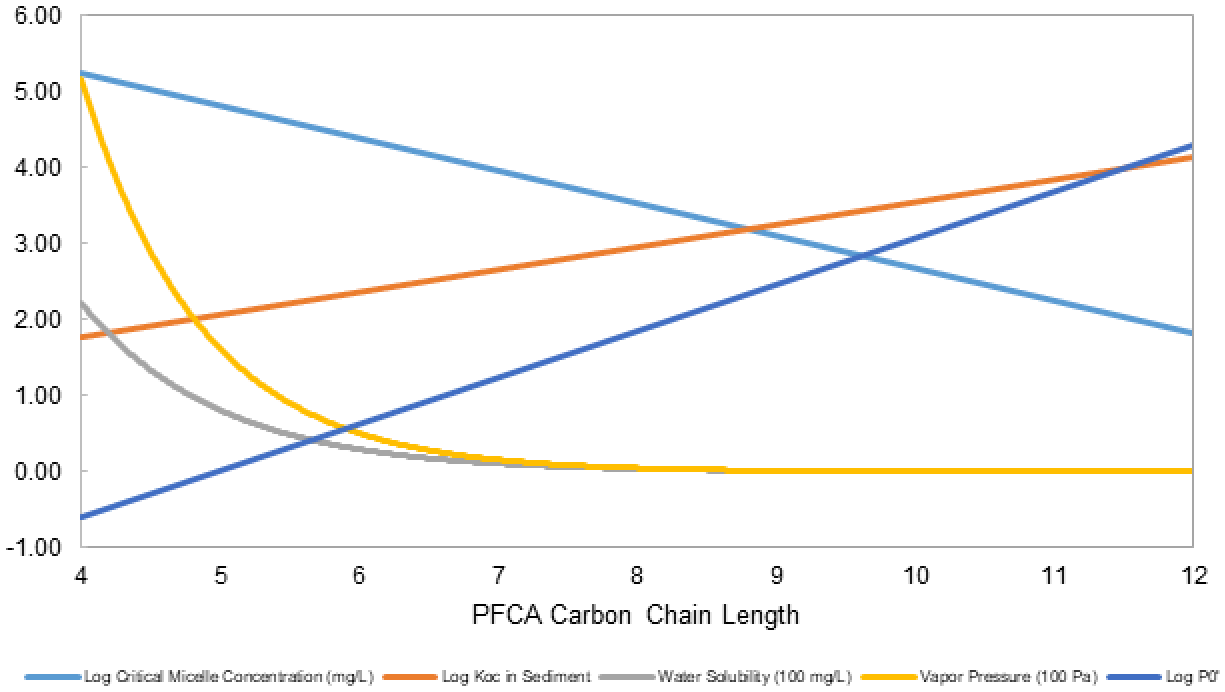

Figure 1. Trends of different PFCAs properties as chain length increases (ITRC, 2023). Water solubility (gray), vapor pressure (yellow), and critical micelle concentration (dark blue) decrease while the K_{oc} (orange) and lipophilicity (light blue) increases (Jing et al., 2009) with chain length.

As seen in Figure 1, these PFCA-property trends are due to the increasing length of the nonpolar fluorocarbon chain length, which would favor nonpolar lipids instead of polar water. The Octanol/Water Partition Coefficient (K_{ow}), commonly used to measure the tendency of a compound to associate with hydrophobic or hydrophilic substances (ITRC 2023), is not very readily used for PFAS chemicals. This is because PFAS chemicals are both hydrophobic and lipophobic and therefore tend to form multiple immiscible layers when added to an octanol/water mixture (Kim et al., 2015). Using “regular” methods to determine the K_{ow} is therefore challenging, which is why the $P^{0'}$was used to measure the lipophilicity of PFCA molecules (Jing et al., 2009).

Additionally, short-chain PFAS interacts with water differently. It has been shown that short-chain PFAS predominates in water, while long-chain PFAS are more prevalent in sediment (Zhao et al., 2016; Bai and Son, 2021). The Organic

Carbon/Water Partition Coefficient (K_{oc}) is a metric used to measure the potential of a dissolved compound to associate with or sorb to organic matter in soil. As can be seen from Figure 1, while both short and long-chain PFAAs have high mobility in water, short-chain PFAS are less likely to partition in sediment than long-chain PFAS (Dalahmeh et al., 2018) as their log(K_{oc})values are much higher (ITRC 2023). This means they are more likely to accumulate in water, increasing their effects on humans drinking the contaminated water. Short-chain PFAS could reach up to 88.8% of the total PFAS concentration in water (Zhao et al., 2016). This is likely due to the decreased hydrophobicity of short-chain PFAS, causing them to be more attracted to the water molecules.

Due to their amphiphilic structure and surfactant attributes, another influential property of PFAS molecules is their critical micelle concentration, the minimum concentration of surfactant above which micelles would form. A greater critical micelle concentration would mean fewer micelles and vice versa. When the concentration of a PFAS is more significant than its critical micelle concentration, it forms micelles, which are structures where the hydrophilic heads “shield” the hydrophobic tails of multiple PFAS molecules, forming spheres of PFAS molecules. These micelles can form in the porous structures of adsorbents, making adsorption a viable solution for the removal of high concentrations of PFAS. Hemi-micelles, which are more linear aggregates, can also form at these adsorbents (Zhang et al., 2011). Long-chain PFAS have a much lower critical micelle concentration than short-chain PFAS (see Figure 2) due to their greater hydrophobicity (Campbell et al., 2009), meaning that they form micelles at much lower concentrations. For this reason, the adsorption capacity for long-chain PFAS is higher than that of short-chain PFAS for most adsorbents (Gagliano et al., 2020), making long-chain PFAS easier to remove.

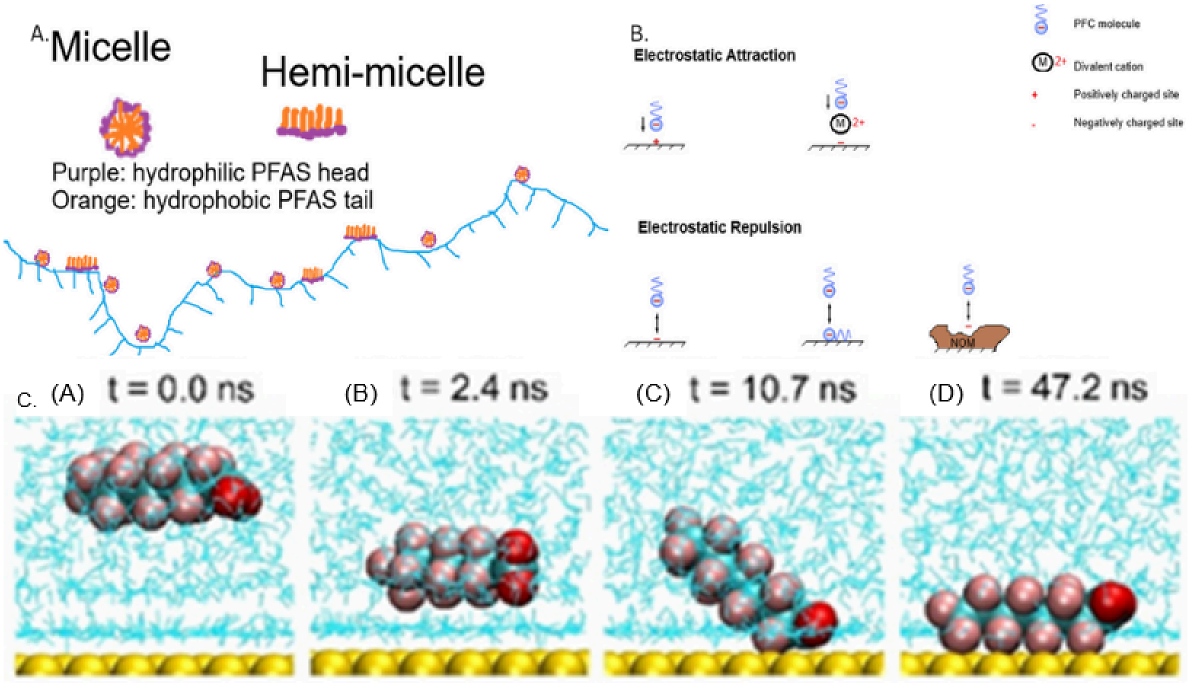

(Zhang et al., 2011; Wang et al., 2023)
Figure 2. A: The formation of micelles and hemi-micelles at high PFAS concentrations on adsorbent material. B: Electrostatic attraction and repulsion in PFAS adsorption. NOM is organic matter. C: Adsorption of PFOA Molecule on Gold Electrode.

In Figure 2C, the electrostatic interactions are between the anionic PFAS molecule and the positively charged gold electrode. The negatively charged PFAS head is attracted to the positively charged gold electrode, resulting in the adsorption of the PFOA molecule onto it.

2.2 PFAS NOMENCLATURE

PFAS molecules consist of a carbon chain of varying length, where at least one of the hydrogen atoms is replaced by a fluorine atom (Buck et al., 2011). PFAS can be divided into perfluoroalkyl carboxylic acids (PFCAs) and perfluoroalkyl sulfonic acids (PFSAs), depending on their functional group (Buck et al., 2011). Two commonly used and studied long-chain PFAS are perfluorooctanoic acid (PFOA) and perfluorooctanesulfonic acid (PFOS). PFOA and PFOS have eight carbons and are a PFCA and a PFSA, respectively. Until it was phased out globally due to its negative health effects, PFOA was commonly used in the textile, leather, and household cleaning agent manufacturing. PFOS was commonly used in Scotchgard, a fabric protector, as well as other stain repellents. However, PFOS has a significantly higher bioaccumulation potential than PFOA, most likely due to the sulfonic acid functional group (Ahrens and Bundschuh, 2014).

Table 2. Different Number of Carbons for Different PFCA and PFSA Compounds and their Designation as Long or Short-Chain ("Naming Conventions for Per- and Polyfluoroalkyl Substances (PFAS)," ITRC)

	Number of Carbons								
PFAS	4	5	6	7	8	9	10	11	12
PFCAs	Short-chain PFCAs				Long-chain PFCAs				
	PFBA	PFPeA	PFHxA	PFHpA	PFOA	PFNA	PFDA	PFUnA	PFDoA
PFSAs	PFBS	PFPeS	PFHxS	PFHpS	PFOS	PFNS	PFDS	PFUnS	PFDoS
	Short-chain PFSAs		Long-chain PFSAs						

In addition to the main functional group (i.e., carboxylic acid versus sulfonic acid), PFAS subclass distinction has been done via chain length. Due to the differences in their properties and resulting removal efficacy, it is essential to note the number of carbons required for classification. According to the Organization for Economic Cooperation and Development, long-chain PFCA compounds consist of eight or more carbons, while long-chain PFSA compounds consist of six or more. Anything below the minimum required carbons is considered a short-chain PFAS compound (OECD/UNEP Global PFC Group, 2013). As seen in Table 2, the naming convention follows the PFXY shorthand, where PF stands for perfluoro, X is the carbon chain length using the hydrocarbon naming convention (e.g., B = 4 carbons for butane, Pe = 5 carbons for pentane), and Y is the functional group (A for carboxylate or S for sulfonate). For example, PFOA stands for perfluorooctanoic acid, and it has 8 carbons (the same naming convention as octane) and a carboxylate functional group.

2.3 COMMON PFAS MOLECULES

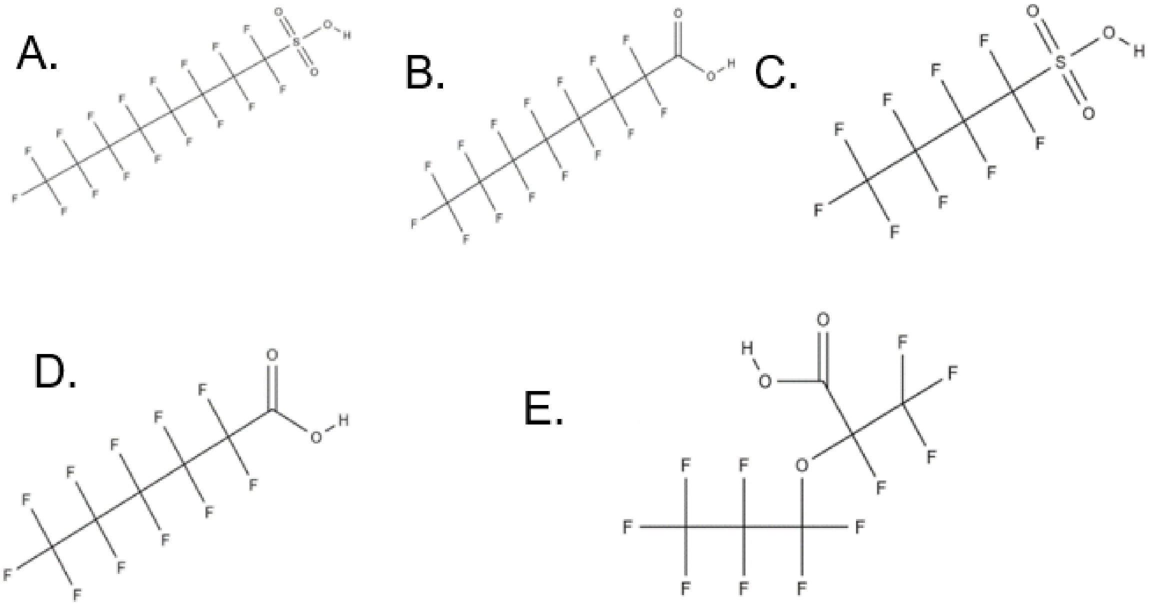

Figure 3. Common PFAS Molecules that will be referenced and explored in detail later in the study: A: PFOS. B: PFOA. C: PFBS. D: PFHxA. E: GenX.

2.3.1. PFOS and PFOA

Perfluorooctanesulfonic acid (PFOS) and Perfluorooctanoic acid (PFOA), as seen in Figures 3A and 3B, respectively, have eight carbons in their chains with a sulfonate group head and carboxylate group head, respectively. They are long-chain PFAS molecules that were two of the most used PFAS compounds before the industry phased them out because of regulations. PFOS was used in Scotchgard, a fabric protector. It was also used in stain-repellent technology. Comparatively, PFOA was commonly used to manufacture textiles, fabrics, leather, and nonstick cookware. Despite their phase-out, both compounds remain widely in the environment due to their stability and accumulative properties. PFOS and PFOA, the oldest PFAS chemicals to date, are also the most well studied PFAS molecules to date because they are two of the most common degradation products from many precursor compounds (Brusseau, 2018).

2.3.2. PFBS

Perfluorobutanesulfonic acid (PFBS), as seen in Figure 3C, has four carbons in its carbon chain with a sulfonate head. It is a short-chain PFAS molecule that has become a replacement to the long-chain PFOS and PFOA used in manufacturing goods such as nonstick cookware, stain repellent, fire retardant, and fabrics. After the leading PFOS producer, 3M, phased out PFOS production, they switched to producing PFBS, resulting in significantly more short-chain compounds in the environment. The concentration of PFBS has been found as high as 6.67 ng/L in the Yellow River (Zhao et. Al, 2016), 0.03-3.4 ng/L in the Pearl River in China (So et al., 2007), and 0.22-153 ng/L in the Rhine River watershed in Europe (Möller et al., 2010). Due to its highly bioaccumulative properties and widespread existence, PFBS is one of the main short-chain PFAS molecules that this paper will focus on in comparing treatment technologies.

2.3.3. PFHxA

Perfluorohexanoic acid (PFHxA), as seen in Figure 3D, has six carbons in its carbon chain with a carboxylate head, making it another increasingly popular short-chain PFAS molecule. PFHxA is commonly used in paper food packaging, stain-resistant fabrics, and photographic film manufacturing. PFHxA has been found to be incredibly dominant in water. In the Truckee River and Las Vegas Wash watersheds outside Las Vegas in 2021, the median concentrations were 6.2 and 74.7 ng/L, respectively (Bai & Son, 2021), and PFHxA was found to be the most dominant species out of all the 17 species tested. In the Cape Fear drainage basin in North Carolina, it was detected at 5.14ng/L (Nakayama et al., 2007). In Rhode Island and New York surface water sources, it was detected at 1.7 ng/L (Zhang et al., 2016). Most notably, it was additionally found to be at 27.8-462 ng/L in Tangxun Lake in China (Zhou et al., 2013) and 0.62-17.4 ng/L in the Rhine River watershed in Europe (Möller et al., 2010). Due to its dominance and presence, PFHxA is a significant contributor to the spread of short-chain PFAS in water worldwide.

2.3.4. GenX

GenX, as seen in Figure 3E, is another of the newer short-chain replacements for PFOA and PFOS. It was developed by Chemours (DuPont) and is currently being used to manufacture the same goods that were made using PFOA and PFOS, such as Teflon and nonstick pans. While its chemical structure is slightly different, its properties are similar to those of its long-chain predecessors, which is a reason why it is a popular replacement. Immediately downstream from a fluorochemical plant in the Merwede River in the Netherlands, its concentration was 800 ng/L, about 13 times the sum of the concentrations of the PFCAs and PFSAs in the water. However, in upstream locations and other sites, the concentration was below the detection limit (0.2 ng/L) (Gebbink et al., 2017). This suggests that point-source removal of GenX could be viable. GenX was also detected in 153 of the 160 surface water samples from China, Europe, Korea, and the US (Pan et al., 2018). Due to its replacement for PFOA and PFOS, GenX is a significant contributor to short-chain PFAS in water worldwide.

See Supplemental Materials Table S2 for the data for concentrations of short-chain PFAS in water.

2.4 EPA HEALTH ADVISORY

Table 3. EPA Health Advisory for Several PFAS Chemicals (EPA, 2022)

PFOA Interim Updated Health Advisory – Input Parameters and HA Value			
Parameter	**Value**	**Units**	**Source**
Chronic RfD	1.50E-09	mg/kg/day	U.S. EPA, 2021a. *Draft* RfD based on developmental immune health outcome (suppression of tetanus vaccine response in 7-year-old children). Human epidemiological studies.
DWI-BW	0.00701	L/kg-day	U.S. EPA, 2019. 90th percentile direct and indirect consumption of community water, consumers-only population, two-day average, for children ages 0 to <5 years based on 2005-2010 National Health and Nutrition Examination Survey (NHANES).
RSC	0.2	N/A	U.S. EPA, 2021a. RSC based on a review of the current scientific literature.
PFOA Interim Updated Health Advisory = 0.004 ppt (EPA 2022a)			

PFOS Interim Updated Health Advisory – Input Parameters and HA Value			
Parameter	**Value**	**Units**	**Source**
Chronic RfD	7.90E-09	mg/kg/day	U.S. EPA, 2021a. *Draft* RfD based on developmental immune health outcome (suppression of diptheria vaccine response in 7-year-old children). Human epidemiological studies.
DWI-BW	0.00701	L/kg-day	U.S. EPA, 2019. 90th percentile direct and indirect consumption of community water, consumers-only population, two-day average, for children ages 0 to <5 years based on 2005-2010 NHANES.
RSC	0.2	N/A	U.S. EPA, 2021a. RSC based on a review of the current scientific literature.
PFOS Interim Updated Health Advisory = 0.02 ppt (EPA 2022b)			

GenX Chemicals Final Health Advisory – Input Parameters and HA Value			
Parameter	**Value**	**Units**	**Source**
Chronic RfD	3.00E-06	mg/kg/day	U.S. EPA, 2021c. Final RfD based on critical liver effects (constellation of liver lesions as defined by the National Toxicology Program Pathology Working Group) in parental female mice exposed to HFPO dimer acid ammonium salt by gavage for 53-64 days.

DWI-BW	0.00469	L/kg-day	U.S. EPA, 2019. 90th percentile two-day average, consumer only estimate of combined direct and indirect community water ingestion for lactating women (13 to <50 years) based on 2005-2010 NHANES.
RSC	0.2	N/A	U.S. EPA, 2021a. RSC based on a review of the current scientific literature.
GenX Interim Updated Health Advisory = 10 ppt (EPA 2022c)			

PFBS Interim Updated Health Advisory – Input Parameters and HA Value			
Parameter	**Value**	**Units**	**Source**
Chronic RfD	3.00E-04	mg/kg/day	U.S. EPA, 2021a. Final RfD based on critical effect of decreased serum total thyroxine (T4) in newborn (postnatal day (PND) 1) mice after gestational exposure to the mother.
DWI-BW	0.0354	L/kg-day	U.S. EPA, 2019. 90th percentile two-day average, consumer only estimate of combined direct and indirect community water ingestion for women of childbearing age (13 to <50 years) based on 2005-2010 NHANES.
RSC	0.2	N/A	U.S. EPA, 2021a. RSC based on a review of the current scientific literature.
PFBS Interim Updated Health Advisory = 2000 ppt (EPA 2022d)			

The health advisories for PFAS chemicals set incredibly low concentrations from 0.004-2000 ppt compared to concentrations found in waterways around the world (Table 3). Due to the bioaccumulative properties of these PFAS chemicals, high relative concentrations of PFAS can be achieved, especially if removal methods are not implemented. The switch to short-chain PFAS used in industry means that in the future, removal of short-chain PFAS is important as concentrations of short-chain PFAS have been detected (see Section 2.2).

3. SHORT-CHAIN PFAS TREATMENT METHODS

Traditional water treatment methods, such as coagulation, flocculation, sedimentation, filtration, biofiltration, oxidation, UV irradiation, and low-pressure membranes, do not sufficiently address PFAS removal (Rahman et al., 2014). Since PFAS bioaccumulates, large concentrations of PFAS could exist in the drinking water supply if specific measures to remove PFAS compounds are not taken. Additionally, breaking apart the C-C bond through biological treatment would produce short-chain PFAS from long-chain PFAS molecules. Currently, granulated activated carbon is the most commonly used and studied method of PFAS removal. However, granulated activated carbon doesn’t remove short-chain PFAS particularly well due to the increasing polarity of the decreased chain length (Riegel et al., 2023). Due to the physical properties of PFAS, other experimental techniques, such as ion exchange treatment, hydrogels, and membranes, are being tested to improve short-chain PFAS removal efficiency.

3.1 ADSORPTION

Adsorption is the mechanism by which the majority of both long- and short-chain PFAS are removed. The predominant forces that govern PFAS adsorption are their electrostatic and hydrophobic interactions with the positively charged adsorbent materials. The negatively charged PFAS head will have strong electrostatic attractions with a positively charged, divalent adsorbent site (Figure 3B). Currently, short-chain PFAS that are being used instead of phased-out PFAS chemicals such as PFOA and PFOS are PFBS (4 carbons) and GenX (6 carbons). It has been hypothesized that due to the decreasing polarity with chain length, short-chain PFAS removal via adsorption may be less efficient than that of long-chain PFAS (Riegel et al., 2023).

As a result, the electrostatic interactions, the molecular structure of the PFAS molecule, and the physical and chemical properties of the adsorbent material are the main factors affecting PFAS adsorption efficiency. The surface functional groups and pore structure of adsorbent materials are important for this adsorption as well because they can prevent the blockages caused by formed micelles in PFAS compounds (Du et al., 2014). Currently, granulated activated carbon is the choice adsorbent material for PFAS. While it is commonly used as a baseline for PFAS removal, it does not remove short-chain PFAS very well (Gagliano et al., 2020) and is not environmentally friendly either (Militao, 2023) as it is coal-based (Figure 4A).

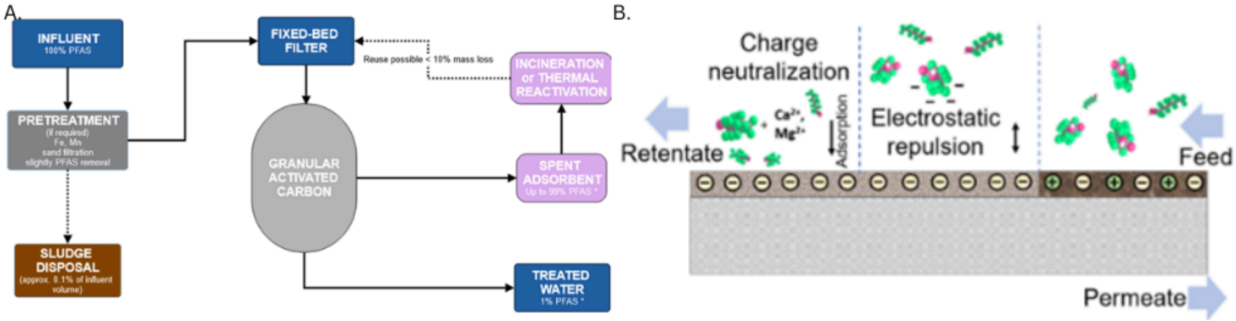

Figure 4. A: Sample GAC PFAS adsorption system (Riegel et al., 2023). GAC is used as baseline for PFAS removal in terms of efficacy and cost. B: Charge Neutralization of PFAS retentate when cations are added (Lee et al., 2022).

3.2 HYDROGELS

Hydrogel-based sorbents are commonly tested for PFAS removal efficacy (Huang et al., 2018) because of their ability to aid the adsorption process. Hydrogels are polymer networks that can absorb large amounts of water (up to 90% in some cases) while maintaining their physical integrity (Gutierrez et al., 2022). The polar, hydrophilic functional groups on the polymer lead to water retention and absorption. Crosslinks between polymer chains prevent dissolution, leading to their stability in solution (Gutierrez et al., 2022). The polar, cationic monomer's properties aid in the adsorption process through positive-negative electrostatic interactions and hydrogen bonding. Hydrogel-based sorbents are highly hydrophilic and therefore can allow pollutants to diffuse into the hydrogels (Huang et al., 2018). In the context of PFAS removal, this means that more PFAS molecules could more easily be adsorbed, leading to a greater removal of short-chain PFAS, which is more difficult to remove than long-chain. Additionally, hydrogels are very inexpensive to produce and also biodegradable, which is important as they can be used widely and sustainably for the water treatment of PFAS-contaminated water (Le et al., 2023).

The poly (*N*-[3-(dimethylamino)propyl]acrylamide (DMAPAA-Q) hydrogel showed promising results for short-chain PFAS adsorption (Ateia et al., 2019). The hydrogel had a surface area of 5.7 m^2 g^{-1} and was tested on several water sources, including surface and wastewater for the purpose of the removal of 16 different PFAS chemicals, including 11 short-chain (C4-7) and 5 long-chain (C8-10). For all of these compounds, the DMAPAA-Q hydrogel had a fast removal with equilibrium being reached in under 2 hours. The removal efficiency for the hydrogel is very high for all PFAS, both short and long-chain, with more than an 80% removal efficiency in distilled, deionized (DDI) water (Figure 5A). Removal efficiency of sulfonic PFAS was found to be higher than carboxylic PFAS regardless of chain length, possibly due to the greater molecular size of the sulfonic PFAS. The removal of the short-chain PFAS specifically is significantly higher here compared to granular activated carbon, which supports the idea that this hydrogel could be a potential replacement as the primary adsorbent material for PFAS removal. A key part of considering hydrogel adsorbents as practical applications is their regeneration. In the same study, regeneration of the DMAPAA-Q hydrogel was tested through adsorption and desorption cycles. Six adsorption/desorption cycles were run, and the performance of the polymer was maintained throughout all cycles as the regeneration percentage remained above 98%.

Alginate hydrogels have also been commonly used to entrap adsorbents such as chitosan for water treatment purposes. The application of *Moringa oleifera* seed powder encapsulated in alginate beads was tested in 2023 (Militao et al., 2023). *Moringa oleifera* is very commonly cultivated in the tropics and sub-tropics, as they are able to survive in harsh conditions (Azad et al., 2015). Potentially, this could be a more environmentally friendly adsorbent as opposed to coal-based GAC. The initial concentrations of PFAS tested in the study were 100 μg/L, which represent environmental concentrations such as that of groundwater. For short-chain PFAS removal, the *Moringa oleifera* alginate beads did not perform well, as the maximum removal percentage for PFBS was under 9%, which is unsatisfactory for any water treatment option. It is likely that because the *Moringa oleifera* alginate beads were negatively charged at neutral pH, they experienced electrostatic repulsion with the short-chain PFBS molecule, thereby reducing the removal efficiency.

A polyethylene glycol diacrylate (PEGDA)-based hydrogel sorbent was also tested (Huang et al., 2018). The hydrophilic PEG backbone was hypothesized to allow for high levels of adsorption and a high PFAS removal efficiency. The PEGDA-based hydrogel sorbent that was functionalized using [2-(methacryloyloxy)ethyl]trimethylammonium chloride solution (MTAC) to create hydrophobic regions and/or attractive electrostatic interactions performed very well, was able to completely sorb PFOA and PFBA within 6 hours, and resulted in a 91 and 78% sorption for PFOS and PFBA, respectively. For GenX, the sorption rate was over 95% (Figure 5B). The regeneration of sorbents was done with a 70% methanol solution containing 1% NaCl. As shown in Figure 5B, more than 90% of the PFAS on the spent sorbent were extracted as well as 84% of GenX. The high desorption rate of the sorbent at above 84% for GenX and 97% for all others tested suggests that it can be regenerated for reuse, which is important for an environmentally friendly and sustainable method of adsorption. In the study, it was found that electrostatically attractive force was the key interactive force in the PFAS sorption on the functionalized PEGDA sorbents, which supports the findings from other studies (Wang et al., 2023). The findings suggest that by having a positive ζ-potential, which indicates the difference in electric potential across the phase boundaries of solids and liquids, of functionalized PEGDA sorbents, would cause the sorption rate to increase. While the ζ-potential of unmodified PEGDA is negative, that of the MTAC-modified PEGDA is positive. Therefore, changing the concentration of MTAC during synthesis could result in a higher ζ-potential of the functionalized PEGDA sorbent, resulting in a higher sorption rate.

PFAS removal with an alginate-encapsulated plant albumin and rice straw-derived biochar was recently tested (Militao et al., 2023). Two treated composites, ammonium sulfate (AS) and diammonium phosphate (DAP) as well as a non-treated (NT) composite were tested. For all three adsorbents, the removal of long-chain PFOS was >80%, and the highest was 99%, achieved by the NT biochar-alginate composite beads. Adsorption of PFOS was very high within 24 hours (Figure 5C). The relative fast reaction kinetics can perhaps be attributed to the increased electrostatic attraction between the long-chain PFOS and the hydrogel compared to the short-chain PFBS. As for the adsorption of the short-chain PFBS, the removal efficiency was not as high only between 26 and 39%. All the adsorbents experienced similar removal rates, with the DAP biochar-alginate achieving the highest removal. As seen in Figure 5C, within 72 hours, the removal of PFBS was insufficient. The study suggested that due to the longer chain length, PFOS experienced stronger hydrophobic interactions and therefore was adsorbed at a higher percentage. Indeed, another study showed that granular activated carbon achieved a PFOS removal efficiency of more than 80% and a PFBS removal of less than 40% with an initial concentration of 100 μg/L (Zhang et al., 2021), which is similar to the results achieved in this paper. Unfortunately, regeneration was not tested in this study to determine the feasibility of this modified hydrogel for long-term PFAS removal.

In another study, cellulose nanocrystals (CNCs) were coated with positively charged, lignin-based, flocculant (Tanfloc) and tested for PFAS removal (Shahid, 2021). Two types of Tanfloc, Tanfloc SH and Tanfloc SG (TFSH and TFSG, respectively), were used to prepare the hydrogel beads in the experiments. All bead systems containing Tanfloc achieved higher removal of KPFBS than the CNC alginate control. However, the removal efficiency of an initial concentration of 250 μM KPFBS was found to be very low with the highest removal rate being 38.2% for the 4% TFSH-CNC hydrogel after two hours (Figure 5D). It was determined that the higher removal from the 4% TSFH-CNC beads was due to the increased content of coated CNCs, resulting in more adsorption sites for the KPFBS. However, due to the low removal rate generally, further optimization of the system is needed. Like the previously mentioned study, regeneration was not tested.

Fluorinated hydrogels were tested on the removal of PFAS from water collected from the Sweeney Water Treatment Plant in Wilmington, NC (Kumarasamy et al., 2020). Fluorophilic sorption and targeted ion exchange were used as complementary strategies for this goal. The highest performing fluorogels were the quaternary fluorogels ranging from amine-containing monomer 2-dimethylaminoethyl methacrylate (DMAEMA) 20-40 wt % at > 80% removal of all PFAS tested with the exception of PFBA. Equilibrium was reached in two hours. Regeneration of the quaternary ionic fluorogel with 20 wt % (IF-20+) was tested and shown to be > 95% for GenX removal within two minutes (Figure 5E).

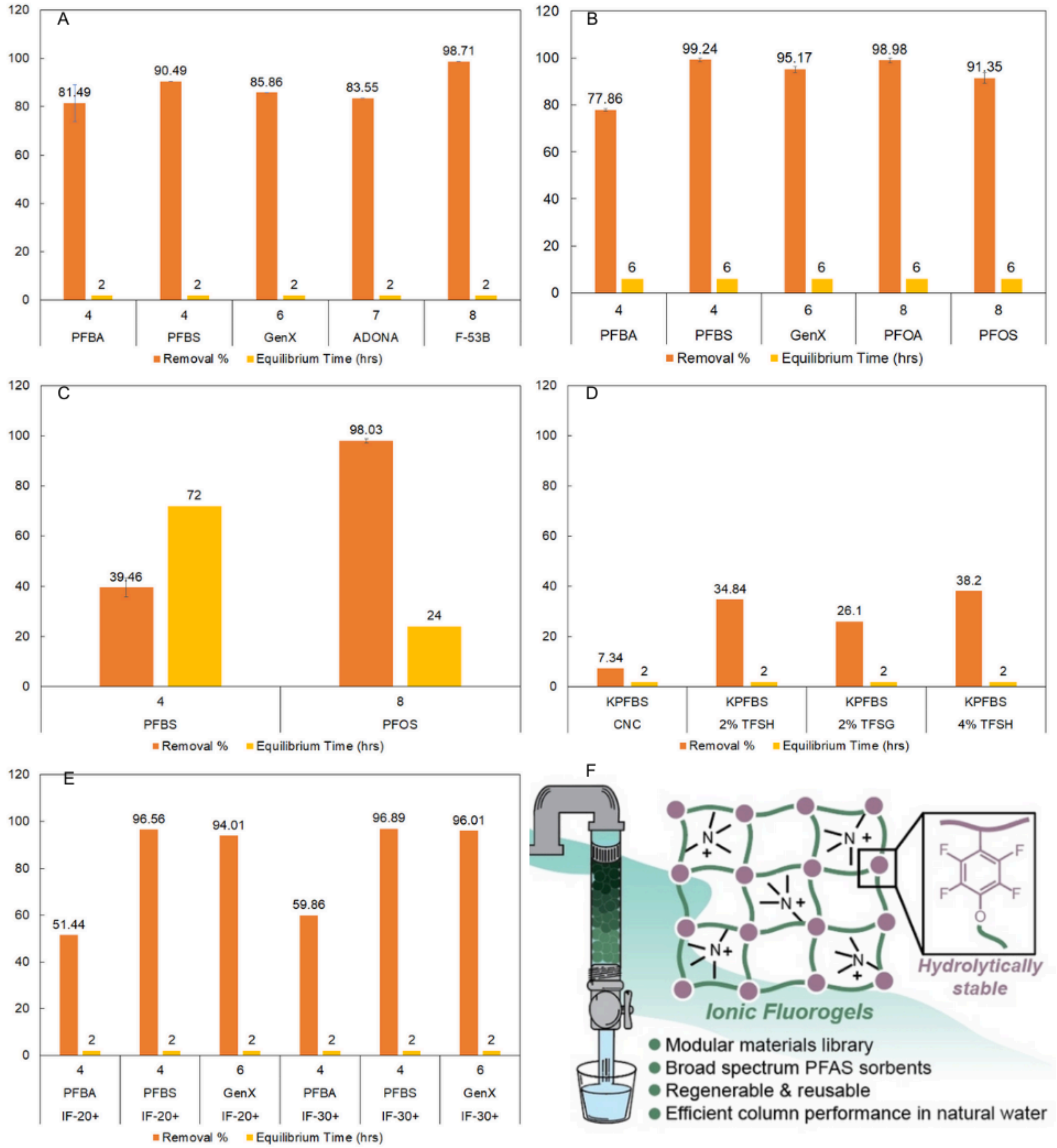
A
81.49
90.49
85.86
83.55
98.71
2
4 PFBA
4 PFBS
6 GenX
7 ADONA
8 F-53B
Removal %
Equilibrium Time (hrs)
B
77.86
99.24
95.17
98.98
91.35
6
4 PFBA
4 PFBS
6 GenX
8 PFOA
8 PFOS
C
39.46
72
98.03
24
4 PFBS
8 PFOS
D
7.34
34.84
26.1
38.2
2
KPFBS CNC
KPFBS 2% TFSH
KPFBS 2% TFSG
KPFBS 4% TFSH
E
51.44
96.56
94.01
59.86
96.89
96.01
2
4 PFBA IF-20+
4 PFBS IF-20+
6 GenX IF-20+
4 PFBA IF-30+
4 PFBS IF-30+
6 GenX IF-30+
0
20
40
60
80
100
120
F
N+
F
O
Hydrolytically stable
Ionic Fluorogels
Modular materials library
Broad spectrum PFAS sorbents
Regenerable & reusable
Efficient column performance in natural water

Figure 5. Removal Efficiency of PFAS by (A) DMAPAA-Q hydrogel (Ateia et al., 2019), (B) PEGDA hydrogel (Huang et al., 2018), (C) Alginate-Encapsulated Plant Albumin and Rice-Straw Derived Biochar Hydrogel (Militao et al., 2023), (D) CNC coated with lignin-based flocculant (Shahid, 2021), and (E) Ionic Fluorogels. IF-X+ corresponds to quaternary ionic fluorogels with X being the wt % (Kumarasamy et al., 2020). (F) Diagram of Ionic fluorogels (Kumarasamy et al., 2020).

3.3 MEMBRANES

Membrane selectivity for PFAS is based on membrane properties such as porosity, pore size, material, and zeta potential (Das and Ronen, 2022). Membranes are typically divided into porous and dense membranes based on their physical characteristics. Membranes with large pore sizes, such as microfiltration or ultrafiltration membranes, performed less efficiently for PFAS separation because of the pore size in comparison to the size of the PFAS compounds (Appleman et al., 2014; Murray et al., 2019).

High-pressure membrane processes using nanoporous membranes such as nanofiltration and nonporous membranes such as reverse osmosis, on the other hand, have been found to be more effective for the separation of PFAS from water (Flores et al., 2013; Pramanik et al., 2017). These membranes work by having pressurized streams enter the membrane, where PFAS particles larger than the pore size would be rejected and water particles smaller than the pore size would go through the membrane. Nanofiltration membranes (NF) have a pore size between 1 nm and 10 nm, allowing more water to permeate than nonporous reverse osmosis (RO) membranes (Lee et al., 2022). Pore size has been shown to have a high impact on PFAS membrane separation (Banks et al., 2020), as shorter-chain and smaller PFAS such as PFBS and PFHxS (300 and 314 g/mol, respectively) had a lower retention rate relatively than long-chain PFAS molecules that were also tested (Banks et al., 2020). A crossflow system would be optimal in order to avoid the accumulation of the solute on the membrane surface over time (Lee et al., 2022). In addition, membrane technology is fully developed, flexible, and scalable, making it potentially a very viable method for PFAS removal. However, a potential downside to these membrane systems is their cost, at \$0.17/m^3 of water for nanofiltration (Jin et al., 2021) and a total cost of \$75,000,000 with an annual cost of \$25,000,000 for a design size of 100 million gallons/day for reverse osmosis treatment (EPA 2024).

There are also electrostatic interactions between PFAS molecules and the membranes themselves. The negatively charged PFAS can experience electrostatic repulsion if faced with a negatively charged membrane surface (Verliefde et al., 2007). These interactions reduce the membrane separation achieved, lowering the PFAS removal efficiency. However, this charge-shielding effect can be neutralized by adding positively charged metallic cations such as Ca^{2+} and Na^+, which cause charge neutralization to the feed water, increasing the affinity for the surface of the membrane

(Figure 2D). The surface area of the membrane also plays a role in the amount of PFAS separation that takes place. It has been shown that increased surface area through increased roughness of the membrane has increased PFAS rejection as there is more area for the PFAS molecules to interact with the membrane (Lin and Cohen, 2011). Many commercial membranes use spiral wound modules as opposed to plate-and-frame modules, thereby increasing the surface area of the membrane. The presence of feed spacers in spiral wound modules contribute to the rough and uneven surface texture while the flat plate membranes arranged in the plate-and-frame configuration lack this roughness. As a result, spiral wound modules are more susceptible to fouling, but their advantages of greater surface area make them efficient options for filtration despite potentially greater maintenance requirements (Lee, 2020).

PFAS removal via an aluminum fumarate (AlFu) metal organic framework (MOF) coated on a hydrophobic polytetrafluoroethylene (PTFE) membrane was tested (Zhang et al., 2022). The study found that for PFSAs with 5 or more carbons, the removal rate was over 90%, while the PFBS (C=4) removal was only 45%. For PFCAs, the removal was between 70-95% for 6-8 carbons, but for PFPeA (C=5), nothing was removed (Figure 6). The removal for long-chain PFAS was greater than that of short-chain PFAS, especially PFBS and PFPeA, most likely due to the larger molecules more easily being rejected by the membrane. A polyacrylonitrile membrane was also tested and found that the removal rate of different PFAS was largely based on chain length (Fang et al., 2024). This is most likely due to the greater size and hydrophobicity of the long-chain PFAS.

In a large study, PFAS removal via an amyloid-carbon hybrid membrane was studied in 2021 (Jin et al., 2021). Twenty six PFAS chemicals were tested, and the results show vast removal for all PFAS. Before treatment, the concentration for all PFAS (except for PFHxS) was 70 ng/L, and all short-and long-chain PFAS except for PFBA were below the detection limits after treatment. For PFBA, the ending concentration was 3.65 ng/L, resulting in a 95% removal rate for PFBA compared to over 99.9% for all the other PFAS tested. Combining traditional activated carbon with amyloid fibrils likely increased the effectiveness because of the highly porous structure of the activated carbon, which led to greater permeability and contact with the amyloid fibrils. A nanofiltration (NF) layer on top of a poly-N-isopropylacrylamide (PNIPAm) pore-functionalized microfiltration support structure was tested to determine the effectiveness of a PNIPAm-coated NF membrane as a combined technique for PFAS removal (Léniz-Pizarro et al., 2022). Due to the expensive and energy-intensive process that is RO, a more sustainable process using combined adsorption and exclusion was tested using the coated NF membrane. Three PFAS were tested: PFOA, PFBA, and GenX. The membrane was partially effective in the removal, with a 70% removal of GenX and PFOA but only a 50% removal of PFBA after 12 hours. The authors of the study hypothesized that with the synthesis of denser NF layers and more tailored functionalization of the PNIPAm, a more sustainable and effective process for PFAS removal could be reached. A $Ti_3C_2T_x$ MXene membrane was tested for short-chain PFAS removal (Ma et al., 2022). The removal of PFHxA and PFHxS from a solution with initial concentrations of 1 µg/L each was 93.07% and 95.5%, respectively, with higher removal at higher initial concentrations. It is hypothesized that the negatively charged membrane surface led to electrostatic repulsion with the negatively charged PFAS, leading to greater rejection. A continuous anionic TpPa-SO_3H covalent organic framework (COF) membrane was tested for PFAS removal (Nguyen et al., 2024). It exhibited a high rejection for both PFOS and PFOA (99% and 95%, respectively) as well as PFBS and PFBA (90% for both).

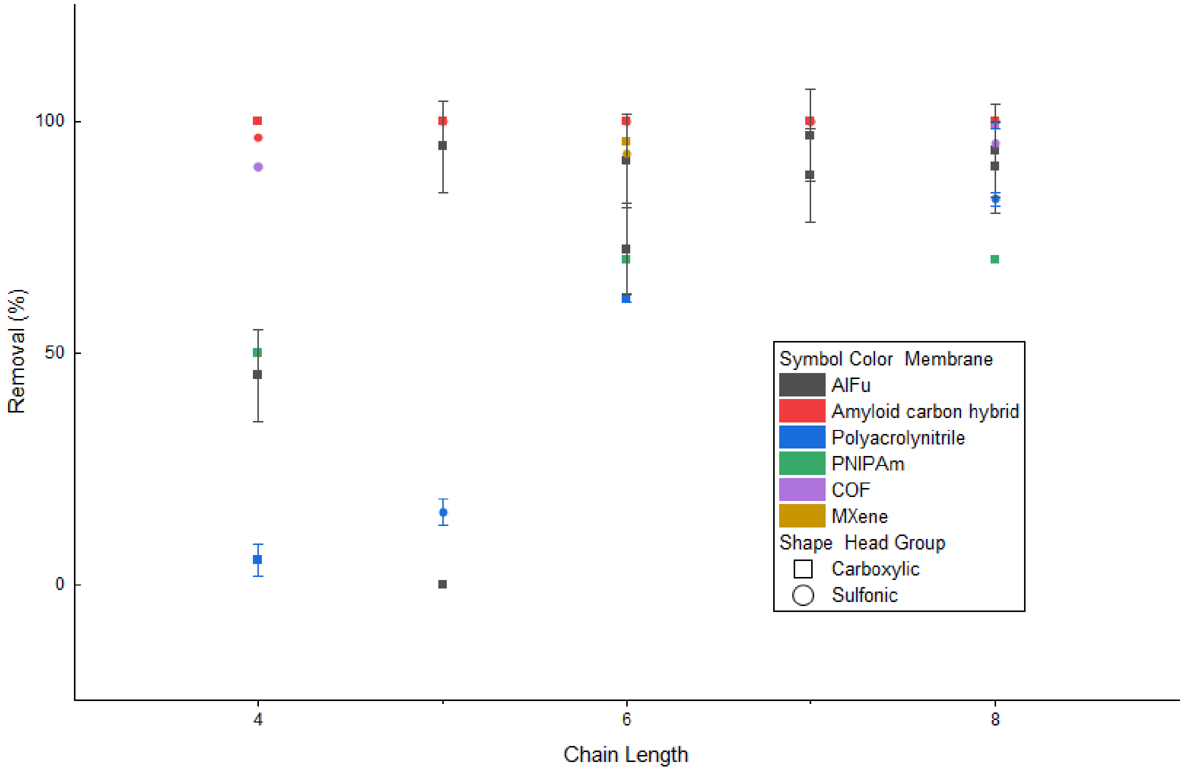

Figure 6. Removal Efficiency of PFAS by membrane technologies (Zhang et al., 2022; Fang et al., 2024; Jin et al., 2021; Léniz-Pizarro et al., 2022; Ma et al., 2022; Nguyen et al., 2024).

4. External Factors

When testing for PFAS removal, many studies test removal in clean, deionized water. However, due to the competition for adsorbent binding sites, the presence of organic matter could have an effect on PFAS removal. Similarly, background anions could also compete for binding sites on the adsorbent material, affecting the PFAS removal. It is also important to test for the effect of pH because as part of the traditional water purification system, the water pH is manipulated. Therefore, understanding the effects of different pH would be important as well in determining which step the technology should be incorporated in, especially in membrane-based treatment systems.

A negatively charged PFAS molecule will experience electrostatic repulsion with a negatively charged adsorbent site and with another already adsorbed negatively charged PFAS molecule, which shows how PFAS molecules can “take up” adsorbent sites and prevent other molecules from adsorbing too. Organic matter that is negatively charged can experience attraction with a positively charged adsorbent material, ultimately resulting in the repulsion with a negatively charged PFAS molecule. In nature, these external factors exist, making removal of PFAS, especially short-chain PFAS, via adsorption much more difficult. Referenced in Figure 4B, when cations are added to the feed mixture, charge neutralization takes place, increasing PFAS affinity to the membrane.

Because PFAS adsorption is primarily governed by the strength of the electrostatic interactions between PFAS molecules and the adsorbent material, changing the ionic strength of the solution could affect adsorption efficiency (Du et al., 2014). Some examples of this would be having other anions in the solution or changing the solution pH, both of which are entirely possible in nature or as part of an existing wastewater treatment solution system. It is hypothesized that due to the increasing hydrophobicity of the long-chain PFAS, the adsorption efficiency increases as long-chain PFAS molecules are less soluble in water as a result (Li et al., 2023). It was also shown that adsorption rate increases with a longer carbon chain length due to a greater molecular size (Appleman et al., 2014). Indeed, pre-adsorbed short-chain PFAS molecules were desorbed by long-chain PFAS molecules in a high density cationic quaternized nanocellulose (Li et al., 2023). Due to the differences in short and long-chain PFAS adsorption efficiency with the same adsorbent material, analyzing specific adsorbent materials solely for short-chain removal is beneficial and necessary.

When tested in solutions with different pH values, the DMAPAA-Q hydrogel maintained its effectiveness with a removal rate of over 80% in all trials regardless of pH or PFAS tested. However, when tested in treated wastewater, the removal efficacy decreased 10-20%, most likely due to the increased presence of background anions from the organic matter competing for adsorbent sites (Figure 7A). Regeneration tested in lake water revealed that adsorption reversibility was not affected by the unclean water, as the adsorption and desorption rates remained near 100% (Ateia et al., 2019). The alginate-encapsulated plant albumin and rice straw-derived biochar was tested in solutions with varying pH values and concentrations of organic matter. Varying the pH between 6 and 8 did not affect the removal efficiency of PFOS nor PFBS. The removal rate of PFOS remained high above 95% while that of PFBS remained low at around 40%. Varying the salt concentration and therefore the ionic strength between 0 M and 0.1 M NaCl did not affect these rates either. Even though the presence of humic acid on adsorbents such as GAC reduced their adsorption efficiency (Kempisty et al., 2022), its presence did not affect the kinetics or the efficiency of the hydrogel (Militao et al., 2023). The ionic fluorogels (Kumarasamy et al., 2020) were tested in wastewater from the Sweeney Water Treatment Plant and were found to be very effective with the exception of PFBA removal most likely due to its short chain length.

The AlFu MOF coated on a hydrophobic PTFE membrane was tested in wastewater, where it achieved a high removal rate for PFSAs with chain lengths greater than 5 but lower removal rates for PFCAs with chain length less than 6. Even though generally PFSAs were more easily removed, no conclusions could be drawn as to whether the AlFu MOF had greater electrostatic affinity to the sulfonic acid versus the carboxylic head group since the AlFu MOF would not preferably adsorb either (Zhang et al., 2022). While the membrane was not tested in DI water, it can be assumed that the removal rate for all PFAS would have been higher in those conditions due to the lack of organic matter. The polyacrylonitrile membrane was tested in solution containing humic acid (Fang et al., 2024), and the removal of PFOS remained high at 98.4% by regulating the membrane pore size to achieve selective interception of the humic acid. Insignificant reduction in PFAS removal was also seen under the effects of versatile NOM and other surfactant competitors. The $Ti_3C_2T_x$ MXene membrane (Ma et al., 2022) was tested in solutions with different pH values, different pressure conditions, and different concentrations of humic acid. At pH values > 7, the membrane is most effective as the electrostatic repulsion of the membrane and the PFAS increases, resulting in the removal rate of 94.55% for PFHxS and 97.58% for PFHxA. However, at low pH values (e.g., pH=3), the removal efficiency decreased rapidly, all the way down to around 30%, indicating that the membrane is best used in alkaline environments. Pressure is another factor that can impact PFAS removal efficiency. At higher pressures of 6 bar, the removal rate dropped 3-4% for both PFAS chemicals (PFHxS and PFHxA) compared to that at lower pressures of 3 bar, most likely due to the increased pressure becoming the dominant separation mechanism (Ma et al., 2022). The effects of organic matter were tested by varying the concentration of humic acid, and as the concentration of humic acid increased, so too did the PFAS removal rate by 2-3%. This was most likely due to the formation of an organic humic acid layer on the membrane, which enhanced the PFAS separation as an additional rejection layer (Figure 7B-D: Ma et al., 2022). The TpPa-SO_3H COF membrane's performance was evaluated with the addition of salts in the feed solution (Figure 7E: Nguyen et al., 2024). When NaCl or Na_2SO_4 was added, the membrane's performance reduced only 4-5% in 2mM salt solution. However, for PFOA, PFBA, and PFBS, the presence of $CaCl_2$ reduced the performance significantly by over 40%. Not every study on the removal of short-chain PFAS chemicals includes experimental results on the impact of pH, ionic background concentration, or presence of organic matter, making it challenging to determine the true ability of the treatment method.

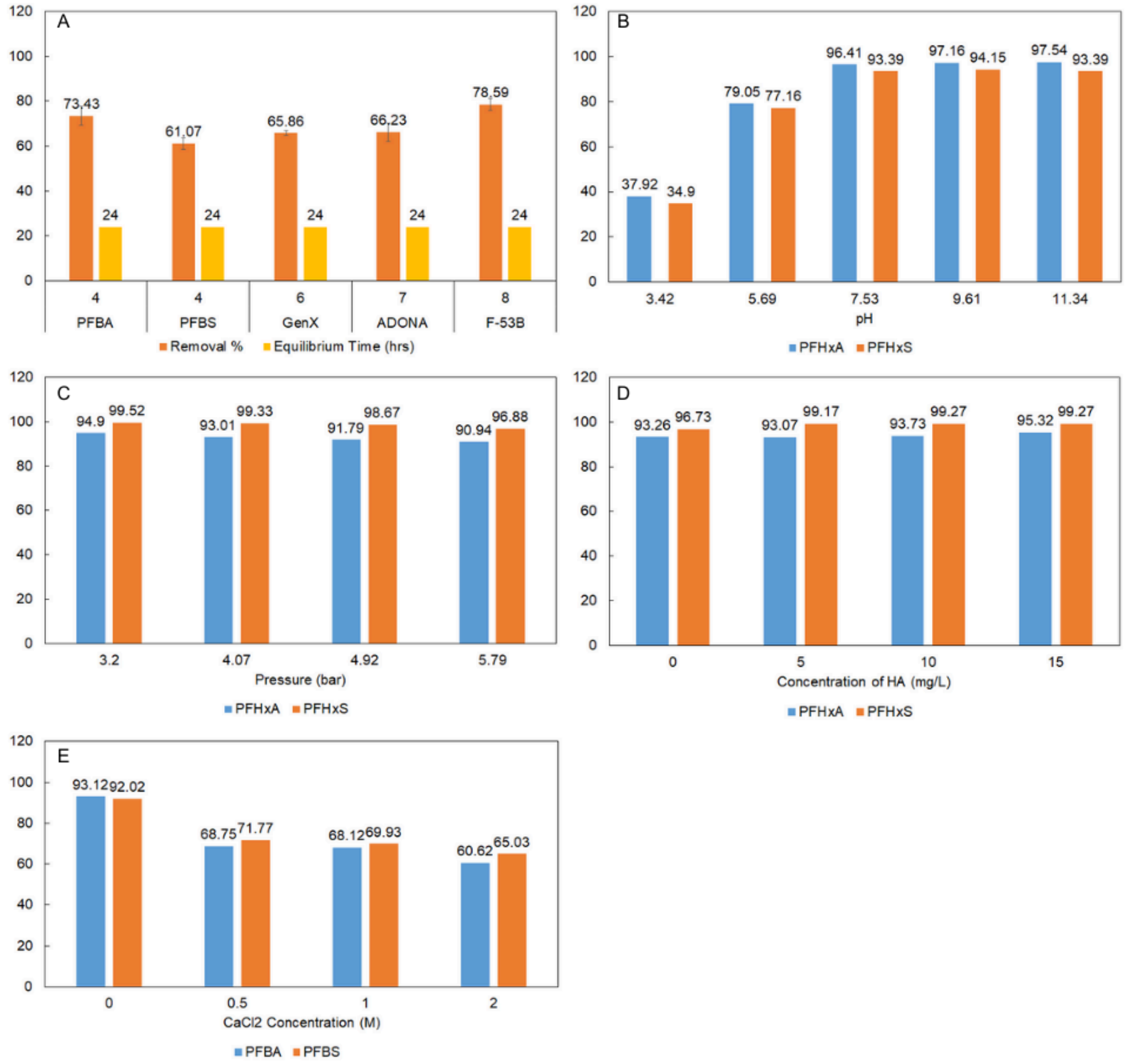

Figure 7. A: Removal Efficiency of PFAS by DMAPAA-Q hydrogel in treated wastewater (Ateia et al., 2019). B-D: Removal Efficiency of PFAS by $Ti_3C_2T_x$ MXene membrane in solutions with varying pH, pressure, and concentration of humic acid (HA), respectively (Ma et al., 2022). E: Removal Efficiency of PFAS by TpPa-SO_3H COF membranes in solutions with varying concentrations of $CaCl_2$ (Nguyen et al., 2024).

5. CONCLUSION

PFAS chemicals have been used since the 1940s for a variety of purposes, including nonstick pans, firefighting foam, and stain repellent. These chemicals have been shown to have numerous health risks, including immunotoxicity, thyroid disease, liver disease and cancer, lipid and insulin dysregulation, kidney disease, uric acid, kidney cancer, and adverse reproductive outcomes. Moreover, due to their chemical stability, they do not biodegrade quickly, hence being known as “forever chemicals.” Their bioaccumulation in water makes them incredibly dangerous, which is why developing techniques to remove and separate PFAS from water is important. Much of the research that has been performed on PFAS has been performed on long-chain PFAS. However, as most companies, such as DuPont and 3M, have switched to using short-chain PFAS such as GenX instead, research needs to be focused on the removal of short-chain PFAS. Many of the techniques that have been found successful in long-chain PFAS removal, such as granular activated carbon adsorption, have been found unsuccessful for short-chain PFAS removal.

The key treatment methods discussed in this review were adsorption and membrane separation. Adsorption is the primary mechanism for numerous hydrogel technologies tested for PFAS removal, and it relies on electrostatic and hydrophobic interactions between the adsorbent material and the PFAS molecule. The best hydrogel technologies were the DMAPAA-Q hydrogel and the ionic fluorogel, and the worst performing hydrogel technologies were the *Moringa Oleifera,* alginate-encapsulated plant albumin, and Tanfloc-coated CNC hydrogel. The best performing hydrogels performed this way likely because they were the most cationic, most positively charged, resulting in greater electrostatic attraction with the short-chain PFAS. However, most of these technologies did not perform well for the shortest-chain PFBA and PFBS (C=4). On the other hand, the membrane technologies performed significantly better, specifically when it came to short-chain PFAS. The best membrane technologies were the amyloid-carbon hybrid membrane, $Ti_3C_2T_x$ MXene membrane, and the TpPa-SO_3H COF membrane. Because NF and RO membrane separation as a technique does not distinguish between short and long-chain PFAS due to the small pore sizes, those membranes generally performed well for short-chain PFAS removal. While these membrane technologies achieved desirable results, more research needs to be done on their feasibility in terms of their price. For example, RO in its entirety has been found to be very expensive despite its proficiency as membrane separation process.

External factors are important to consider when it comes to PFAS removal because in real-world treatment systems, PFAS removal is not attempted from distilled, deionized water. The presence of organic matter, background anions, and different pH values can all affect PFAS removal due to competition for adsorbent sites. Overall, pH values do not have a significant effect on PFAS removal for most hydrogel and membrane technologies, with the only exception being the $Ti_3C_2T_x$ MXene membrane, which fared much better at higher pH values because the MXene surface became negatively charged, resulting in greater electrostatic rejection between the membrane and the short-chain PFAS. The presence of anions did have a negative effect on some treatment technologies, which is important to note. Testing in non-distilled, deionized water had a negative effect when it came to hydrogel technologies, but for membranes, testing in wastewater did not dramatically reduce the removal rate because the membranes did not primarily rely on electrostatic interactions for separation. Many technologies did not test in alternative conditions, and an opportunity for further research would be testing the amyloid-carbon hybrid membrane in wastewater, feedwater with varying ionic concentrations, and solutions across the pH range. While that membrane performed exceptionally in distilled water, it was not tested in alternative conditions. PFAS removal is an issue that needs to be addressed with more research, especially as more and more of it is produced and emitted into the environment.

References

1. 3M's $10 Billion PFAS Deal Approved by Court as Rule Looms (2) [WWW Document], n.d. URL https://news.bloomberglaw.com/environment-and-energy/3ms-10-billion-pfas-deal-approved-by-court-as-rule-looms (accessed 4.17.24).
2. 4 Physical and Chemical Properties – PFAS — Per- and Polyfluoroalkyl Substances [WWW Document], n.d. URL https://pfas-1.itrcweb.org/4-physical-and-chemical-properties/ (accessed 4.15.24).
3. Ahrens, L., Bundschuh, M., 2014. Fate and effects of poly- and perfluoroalkyl substances in the aquatic environment: A review. Environmental Toxicology and Chemistry 33, 1921–1929. https://doi.org/10.1002/etc.2663
4. Alves, A.V., Tsianou, M., Alexandridis, P., 2020. Fluorinated Surfactant Adsorption on Mineral Surfaces: Implications for PFAS Fate and Transport in the Environment. Surfaces 3, 516–566. https://doi.org/10.3390/surfaces3040037
5. Appleman, T.D., Higgins, C.P., Quiñones, O., Vanderford, B.J., Kolstad, C., Zeigler-Holady, J.C., Dickenson, E.R.V., 2014. Treatment of poly- and perfluoroalkyl substances in U.S. full-scale water treatment systems. Water Research 51, 246–255. https://doi.org/10.1016/j.watres.2013.10.067
6. Ateia, M., Arifuzzaman, M., Pellizzeri, S., Attia, M.F., Tharayil, N., Anker, J.N., Karanfil, T., 2019. Cationic polymer for selective removal of GenX and short-chain PFAS from surface waters and wastewaters at ng/L levels. Water Research 163, 114874. https://doi.org/10.1016/j.watres.2019.114874
7. Azad, A.K., Rasul, M.G., Khan, M.M.K., Sharma, S.C., Islam, R., 2015. Prospect of Moringa Seed Oil as a Sustainable Biodiesel Fuel in Australia: A Review. Procedia Engineering 105, 601–606. https://doi.org/10.1016/j.proeng.2015.05.037
8. Bai, X., Son, Y., 2021. Perfluoroalkyl substances (PFAS) in surface water and sediments from two urban watersheds in Nevada, USA. Science of The Total Environment 751, 141622. https://doi.org/10.1016/j.scitotenv.2020.141622
9. Banks, D., Jun, B.-M., Heo, J., Her, N., Park, C.M., Yoon, Y., 2020. Selected advanced water treatment technologies for perfluoroalkyl and polyfluoroalkyl substances: A review. Separation and Purification Technology 231, 115929. https://doi.org/10.1016/j.seppur.2019.115929
10. Bentel, M.J., Yu, Y., Xu, L., Li, Z., Wong, B.M., Men, Y., Liu, J., 2019. Defluorination of Per- and Polyfluoroalkyl Substances (PFASs) with Hydrated Electrons: Structural Dependence and Implications to PFAS Remediation and Management. Environ. Sci. Technol. 53, 3718–3728. https://doi.org/10.1021/acs.est.8b06648
11. Blum, A., Balan, S.A., Scheringer, M., Trier, X., Goldenman, G., Cousins, I.T., Diamond, M., Fletcher, T., Higgins, C., Lindeman, A.E., Peaslee, G., de Voogt, P., Wang, Z., Weber, R., 2015. The Madrid Statement on Poly- and Perfluoroalkyl

Substances (PFASs). Environmental Health Perspectives 123, A107–A111. https://doi.org/10.1289/ehp.1509934

12. Brusseau, M.L., 2018. Assessing the potential contributions of additional retention processes to PFAS retardation in the subsurface. Science of The Total Environment 613–614, 176–185. https://doi.org/10.1016/j.scitotenv.2017.09.065
13. Buck, R.C., Franklin, J., Berger, U., Conder, J.M., Cousins, I.T., de Voogt, P., Jensen, A.A., Kannan, K., Mabury, S.A., van Leeuwen, S.P., 2011. Perfluoroalkyl and polyfluoroalkyl substances in the environment: Terminology, classification, and origins. Integrated Environmental Assessment and Management 7, 513–541. https://doi.org/10.1002/ieam.258
14. Campbell, T.Y., Vecitis, C.D., Mader, B.T., Hoffmann, M.R., 2009. Perfluorinated Surfactant Chain-Length Effects on Sonochemical Kinetics. J. Phys. Chem. A 113, 9834–9842. https://doi.org/10.1021/jp903003w
15. Chen, X., Vanangamudi, A., Wang, J., Jegatheesan, J., Mishra, V., Sharma, R., Gray, S.R., Kujawa, J., Kujawski, W., Wicaksana, F., Dumée, L.F., 2020. Direct contact membrane distillation for effective concentration of perfluoroalkyl substances – Impact of surface fouling and material stability. Water Research 182, 116010. https://doi.org/10.1016/j.watres.2020.116010
16. Country information - OECD Portal on Per and Poly Fluorinated Chemicals [WWW Document], n.d. URL https://www.oecd.org/chemicalsafety/portal-perfluorinated-chemicals/countryinformation/european-union.htm (accessed 4.17.24).
17. Dalahmeh, S., Tirgani, S., Komakech, A.J., Niwagaba, C.B., Ahrens, L., 2018. Per- and polyfluoroalkyl substances (PFASs) in water, soil and plants in wetlands and agricultural areas in Kampala, Uganda. Science of The Total Environment 631–632, 660–667. https://doi.org/10.1016/j.scitotenv.2018.03.024
18. Daly, E.R., Chan, B.P., Talbot, E.A., Nassif, J., Bean, C., Cavallo, S.J., Metcalf, E., Simone, K., Woolf, A.D., 2018. Per- and polyfluoroalkyl substance (PFAS) exposure assessment in a community exposed to contaminated drinking water, New Hampshire, 2015. International Journal of Hygiene and Environmental Health 221, 569–577. https://doi.org/10.1016/j.ijheh.2018.02.007
19. Das, S., Ronen, A., 2022. A Review on Removal and Destruction of Per- and Polyfluoroalkyl Substances (PFAS) by Novel Membranes. Membranes 12, 662. https://doi.org/10.3390/membranes12070662
20. Du, Z., Deng, S., Bei, Y., Huang, Q., Wang, B., Huang, J., Yu, G., 2014. Adsorption behavior and mechanism of perfluorinated compounds on various adsorbents—A review. Journal of Hazardous Materials 274, 443–454. https://doi.org/10.1016/j.jhazmat.2014.04.038
21. Fang, F., Chen, S., Shi, K., Xu, S., Yi, Z., Lei, L., Zhuang, L., Wan, H., Xu, Z., 2024. Hydrophilic membranes for effective removal of PFAS from water: Anti-fouling,

durability, and reusability. Separation and Purification Technology 348, 127379. https://doi.org/10.1016/j.seppur.2024.127379

22. Fenton, S.E., Ducatman, A., Boobis, A., DeWitt, J.C., Lau, C., Ng, C., Smith, J.S., Roberts, S.M., 2021. Per- and Polyfluoroalkyl Substance Toxicity and Human Health Review: Current State of Knowledge and Strategies for Informing Future Research. Environmental Toxicology and Chemistry 40, 606–630. https://doi.org/10.1002/etc.4890
23. Flores, C., Ventura, F., Martin-Alonso, J., Caixach, J., 2013. Occurrence of perfluorooctane sulfonate (PFOS) and perfluorooctanoate (PFOA) in N.E. Spanish surface waters and their removal in a drinking water treatment plant that combines conventional and advanced treatments in parallel lines. Science of The Total Environment 461–462, 618–626. https://doi.org/10.1016/j.scitotenv.2013.05.026
24. Gagliano, E., Sgroi, M., Falciglia, P.P., Vagliasindi, F.G.A., Roccaro, P., 2020. Removal of poly- and perfluoroalkyl substances (PFAS) from water by adsorption: Role of PFAS chain length, effect of organic matter and challenges in adsorbent regeneration. Water Research 171, 115381. https://doi.org/10.1016/j.watres.2019.115381
25. Gebbink, W.A., van Asseldonk, L., van Leeuwen, S.P.J., 2017. Presence of Emerging Per- and Polyfluoroalkyl Substances (PFASs) in River and Drinking Water near a Fluorochemical Production Plant in the Netherlands. Environ. Sci. Technol. 51, 11057–11065. https://doi.org/10.1021/acs.est.7b02488
26. Glüge, J., Scheringer, M., Cousins, I.T., DeWitt, J.C., Goldenman, G., Herzke, D., Lohmann, R., Ng, C.A., Trier, X., Wang, Z., 2020. An overview of the uses of per- and polyfluoroalkyl substances (PFAS). Environ. Sci.: Processes Impacts 22, 2345–2373. https://doi.org/10.1039/D0EM00291G
27. Gujjala, L.K.S., Won, W., 2022. Process development, techno-economic analysis and life-cycle assessment for laccase catalyzed synthesis of lignin hydrogel. Bioresource Technology 364, 128028. https://doi.org/10.1016/j.biortech.2022.128028
28. Gutierrez, A.M., Frazar, E.M., Klaus, M.V.X., Paul, P., Hilt, J.Z., 2022. Hydrogels and Hydrogel Nanocomposites: Enhancing Healthcare Through Human and Environmental Treatment. Adv Healthc Mater 11, e2101820. https://doi.org/10.1002/adhm.202101820
29. Heydebreck, F., Tang, J., Xie, Z., Ebinghaus, R., 2015. Alternative and Legacy Perfluoroalkyl Substances: Differences between European and Chinese River/Estuary Systems. Environ. Sci. Technol. 49, 8386–8395. https://doi.org/10.1021/acs.est.5b01648
30. Hill, P.J., Taylor, M., Goswami, P., Blackburn, R.S., 2017. Substitution of PFAS chemistry in outdoor apparel and the impact on repellency performance. Chemosphere 181, 500–507. https://doi.org/10.1016/j.chemosphere.2017.04.122

31. Huang, P.-J., Hwangbo, M., Chen, Z., Liu, Y., Kameoka, J., Chu, K.-H., 2018. Reusable Functionalized Hydrogel Sorbents for Removing Long- and Short-Chain Perfluoroalkyl Acids (PFAAs) and GenX from Aqueous Solution. ACS Omega 3, 17447–17455. https://doi.org/10.1021/acsomega.8b02279
32. Jeon, S., Lee, E., Min, T., Lee, Y., Lee, G., Kim, A., Yoon, H., 2024. Efficient removal of short-chain perfluoroalkyl substances (PFAS) using asymmetric membrane capacitive deionization. Separation and Purification Technology 348, 127728. https://doi.org/10.1016/j.seppur.2024.127728
33. Jin, T., Peydayesh, M., Joerss, H., Zhou, J., Bolisetty, S., Mezzenga, R., 2021. Amyloid fibril-based membranes for PFAS removal from water. Environmental Science: Water Research & Technology 7, 1873–1884. https://doi.org/10.1039/D1EW00373A
34. Jing, P., Rodgers, P.J., Amemiya, S., 2009. High Lipophilicity of Perfluoroalkyl Carboxylate and Sulfonate: Implications for Their Membrane Permeability. J. Am. Chem. Soc. 131, 2290–2296. https://doi.org/10.1021/ja807961s
35. Kempisty, D.M., Arevalo, E., Spinelli, A.M., Edeback, V., Dickenson, E.R.V., Husted, C., Higgins, C.P., Summers, R.S., Knappe, D.R.U., 2022. Granular activated carbon adsorption of perfluoroalkyl acids from ground and surface water. AWWA Water Science 4, e1269. https://doi.org/10.1002/aws2.1269
36. Kim, M., Li, L.Y., Grace, J.R., Yue, C., 2015. Selecting reliable physicochemical properties of perfluoroalkyl and polyfluoroalkyl substances (PFASs) based on molecular descriptors. Environmental Pollution 196, 462–472. https://doi.org/10.1016/j.envpol.2014.11.008
37. Kirsch, P., 2013. Modern fluoroorganic chemistry: synthesis, reactivity, applications. John Wiley & Sons.
38. Kucharzyk, K. (Kate), Darlington, R., Benotti, M., Deeb, R., Hawley, E., 2017. Novel treatment technologies for PFAS compounds: A critical review. Journal of Environmental Management 204. https://doi.org/10.1016/j.jenvman.2017.08.016
39. Kumarasamy, E., Manning, I.M., Collins, L.B., Coronell, O., Leibfarth, F.A., 2020. Ionic Fluorogels for Remediation of Per- and Polyfluorinated Alkyl Substances from Water. ACS Cent. Sci. 6, 487–492. https://doi.org/10.1021/acscentsci.9b01224
40. Ladapo, J.A., 2019. Review of GenX Pollution: GenX Pollution of the Cape Fear River in North Carolina, U.S.A. 15.
41. Le, V.T., Joo, S.-W., Berkani, M., Mashifana, T., Kamyab, H., Wang, C., Vasseghian, Y., 2023. Sustainable cellulose-based hydrogels for water treatment and purification. Industrial Crops and Products 205, 117525. https://doi.org/10.1016/j.indcrop.2023.117525
42. Lee, S., 2020. Performance Comparison of Spiral-Wound and Plate-and-Frame Forward Osmosis Membrane Module. Membranes 10, 318. https://doi.org/10.3390/membranes10110318

43. Lee, T., Speth, T.F., Nadagouda, M.N., 2022. High-pressure membrane filtration processes for separation of Per- and polyfluoroalkyl substances (PFAS). Chemical Engineering Journal 431, 134023. https://doi.org/10.1016/j.cej.2021.134023
44. Léniz-Pizarro, F., Vogler, R.J., Sandman, P., Harris, N., Ormsbee, L.E., Liu, C., Bhattacharyya, D., 2022. Dual-Functional Nanofiltration and Adsorptive Membranes for PFAS and Organics Separation from Water. ACS ES T Water 2, 863–872. https://doi.org/10.1021/acsestwater.2c00043
45. Leung, S.C.E., Wanninayake, D., Chen, D., Nguyen, N.-T., Li, Q., 2023. Physicochemical properties and interactions of perfluoroalkyl substances (PFAS) - Challenges and opportunities in sensing and remediation. Science of The Total Environment 905, 166764. https://doi.org/10.1016/j.scitotenv.2023.166764
46. Li, D., Lee, C.-S., Zhang, Y., Das, R., Akter, F., Venkatesan, A.K., Hsiao, B.S., 2023. Efficient removal of short-chain and long-chain PFAS by cationic nanocellulose. J. Mater. Chem. A 11, 9868–9883. https://doi.org/10.1039/D3TA01851B
47. Lin, N.H., Cohen, Y., 2011. QCM study of mineral surface crystallization on aromatic polyamide membrane surfaces. Journal of Membrane Science 379, 426–433. https://doi.org/10.1016/j.memsci.2011.06.018
48. Lindstrom, A.B., Strynar, M.J., Libelo, E.L., 2011. Polyfluorinated Compounds: Past, Present, and Future. Environ. Sci. Technol. 45, 7954–7961. https://doi.org/10.1021/es2011622
49. Ma, J., Wang, Y., Xu, H., Ding, M., Gao, L., 2022. MXene (Ti3T2CX)-reinforced thin-film polyamide nanofiltration membrane for short-chain perfluorinated compounds removal. Process Safety and Environmental Protection 168, 275–284. https://doi.org/10.1016/j.psep.2022.09.080
50. Militao, I.M., 2023. Developing alginate-based hydrogel adsorbents for PFAS removal from water systems.
51. Militao, I.M., Roddick, F., Fan, L., Zepeda, L.C., Parthasarathy, R., Bergamasco, R., 2023. PFAS removal from water by adsorption with alginate-encapsulated plant albumin and rice straw-derived biochar. Journal of Water Process Engineering 53, 103616. https://doi.org/10.1016/j.jwpe.2023.103616
52. Möller, A., Ahrens, L., Surm, R., Westerveld, J., van der Wielen, F., Ebinghaus, R., de Voogt, P., 2010. Distribution and sources of polyfluoroalkyl substances (PFAS) in the River Rhine watershed. Environmental Pollution 158, 3243–3250. https://doi.org/10.1016/j.envpol.2010.07.019
53. Munoz, G., Liu, J., Vo Duy, S., Sauvé, S., 2019. Analysis of F-53B, Gen-X, ADONA, and emerging fluoroalkylether substances in environmental and biomonitoring samples: A review. Trends in Environmental Analytical Chemistry 23, e00066. https://doi.org/10.1016/j.teac.2019.e00066
54. Murray, C.C., Vatankhah, H., McDonough, C.A., Nickerson, A., Hedtke, T.T., Cath, T.Y., Higgins, C.P., Bellona, C.L., 2019. Removal of per- and polyfluoroalkyl

substances using super-fine powder activated carbon and ceramic membrane filtration. Journal of Hazardous Materials 366, 160–168. https://doi.org/10.1016/j.jhazmat.2018.11.050

55. Nakayama, S., Strynar, M.J., Helfant, L., Egeghy, P., Ye, X., Lindstrom, A.B., 2007. Perfluorinated Compounds in the Cape Fear Drainage Basin in North Carolina. Environ. Sci. Technol. 41, 5271–5276. https://doi.org/10.1021/es070792y

56. Naming Conventions for Per- and Polyfluoroalkyl Substances (PFAS), n.d.

57. Nguyen, T.-T., Min, X., Xia, W., Qiang, Z., Khandge, R.S., Yu, H.-K., Wang, J.-W., Wang, Y., Ma, X., 2024. Anionic covalent organic framework membranes for the removal of per- and polyfluoroalkyl substances with enhanced selectivity. Journal of Membrane Science 705, 122925. https://doi.org/10.1016/j.memsci.2024.122925

58. Pan, Y., Zhang, H., Cui, Q., Sheng, N., Yeung, L.W.Y., Sun, Y., Guo, Y., Dai, J., 2018. Worldwide Distribution of Novel Perfluoroether Carboxylic and Sulfonic Acids in Surface Water. Environ. Sci. Technol. 52, 7621–7629. https://doi.org/10.1021/acs.est.8b00829

59. Pramanik, B.K., Pramanik, S.K., Sarker, D.C., Suja, F., 2017. Removal of emerging perfluorooctanoic acid and perfluorooctane sulfonate contaminants from lake water. Environmental Technology 38, 1937–1942. https://doi.org/10.1080/09593330.2016.1240716

60. Qiu, T., Davies, P.A., 2012. Comparison of Configurations for High-Recovery Inland Desalination Systems. Water 4, 690–706. https://doi.org/10.3390/w4030690

61. Rahman, M.F., Peldszus, S., Anderson, W.B., 2014. Behaviour and fate of perfluoroalkyl and polyfluoroalkyl substances (PFASs) in drinking water treatment: A review. Water Research 50, 318–340. https://doi.org/10.1016/j.watres.2013.10.045

62. Rayne, S., Forest, K., 2009. Perfluoroalkyl sulfonic and carboxylic acids: A critical review of physicochemical properties, levels and patterns in waters and wastewaters, and treatment methods. Journal of Environmental Science and Health, Part A 44, 1145–1199. https://doi.org/10.1080/10934520903139811

63. Riegel, M., Egner, S., Sacher, F., Beuthe, B., Bonte, M., Hjort, M., 2020. Review of water treatment systems for PFAS removal.

64. Riegel, M., Haist-Gulde, B., Sacher, F., 2023. Sorptive removal of short-chain perfluoroalkyl substances (PFAS) during drinking water treatment using activated carbon and anion exchanger. Environ Sci Eur 35, 1–12. https://doi.org/10.1186/s12302-023-00716-5

65. Shahid, I., n.d. Nanocellulose-based systems for the removal of perfluoroalkyl compounds from water.

66. So, M.K., Miyake, Y., Yeung, W.Y., Ho, Y.M., Taniyasu, S., Rostkowski, P., Yamashita, N., Zhou, B.S., Shi, X.J., Wang, J.X., Giesy, J.P., Yu, H., Lam, P.K.S., 2007. Perfluorinated compounds in the Pearl River and Yangtze River of China. Chemosphere 68, 2085–2095. https://doi.org/10.1016/j.chemosphere.2007.02.008

67. Sun, M., Arevalo, E., Strynar, M., Lindstrom, A., Richardson, M., Kearns, B., Pickett, A., Smith, C., Knappe, D.R.U., 2016. Legacy and Emerging Perfluoroalkyl Substances Are Important Drinking Water Contaminants in the Cape Fear River Watershed of North Carolina. Environ. Sci. Technol. Lett. 3, 415–419. https://doi.org/10.1021/acs.estlett.6b00398
68. Thompson, K.A., Ray, H., Gerrity, D., Quiñones, O., Dano, E., Prieur, J., Vanderford, B., Steinle-Darling, E., Dickenson, E.R.V., 2024. Sources of Per- and Polyfluoroalkyl Substances in an Arid, Urban, Wastewater-Dominated Watershed. https://doi.org/10.2139/ssrn.4717797
69. US EPA, O., 2016. PFAS Explained [WWW Document]. URL https://www.epa.gov/pfas/pfas-explained (accessed 3.25.24).
70. US EPA, O., 2015. Long-Chain Perfluoroalkyl Carboxylate (LCPFAC) Chemicals [WWW Document]. URL https://www.epa.gov/assessing-and-managing-chemicals-under-tsca/long-chain-perfluoroalkyl-carboxylate-lcpfac-chemicals (accessed 4.17.24).
71. Verliefde, A.R.D., Heijman, S.G.J., Cornelissen, E.R., Amy, G., Van Der Bruggen, B., Van Dijk, J.C., 2007. Influence of electrostatic interactions on the rejection with NF and assessment of the removal efficiency during NF/GAC treatment of pharmaceutically active compounds in surface water. Water Research 41, 3227–3240. https://doi.org/10.1016/j.watres.2007.05.022
72. Wang, X., Ham, S., Zhang, H., Wang, Y., Qiao, R., 2023. Adsorption of Model Polyfluoroalkyl Substances on Gold Electrodes for Electroanalytical Applications. ChemElectroChem 10. https://doi.org/10.1002/celc.202300298
73. Zhang, D., He, Q., Wang, M., Zhang, W., Liang, Y., 2021. Sorption of perfluoroalkylated substances (PFASs) onto granular activated carbon and biochar. Environmental Technology 42, 1798–1809. https://doi.org/10.1080/09593330.2019.1680744
74. Zhang, J., Huang, Z., Gao, L., Gray, S., Xie, Z., 2022. Study of MOF incorporated dual layer membrane with enhanced removal of ammonia and per-/poly-fluoroalkyl substances (PFAS) in landfill leachate treatment. Science of The Total Environment 806, 151207. https://doi.org/10.1016/j.scitotenv.2021.151207
75. Zhang, Q., Deng, S., Yu, G., Huang, J., 2011. Removal of perfluorooctane sulfonate from aqueous solution by crosslinked chitosan beads: Sorption kinetics and uptake mechanism. Bioresource Technology 102, 2265–2271. https://doi.org/10.1016/j.biortech.2010.10.040
76. Zhang, X., Lohmann, R., Dassuncao, C., Hu, X.C., Weber, A.K., Vecitis, C.D., Sunderland, E.M., 2016. Source Attribution of Poly- and Perfluoroalkyl Substances (PFASs) in Surface Waters from Rhode Island and the New York Metropolitan Area. Environ. Sci. Technol. Lett. 3, 316–321. https://doi.org/10.1021/acs.estlett.6b00255

77. Zhao, P., Xia, X., Dong, J., Xia, N., Jiang, X., Li, Y., Zhu, Y., 2016. Short- and long-chain perfluoroalkyl substances in the water, suspended particulate matter, and surface sediment of a turbid river. Science of The Total Environment 568, 57–65. https://doi.org/10.1016/j.scitotenv.2016.05.221

78. Zhao, Z., Cheng, X., Hua, X., Jiang, B., Tian, C., Tang, J., Li, Q., Sun, H., Lin, T., Liao, Y., Zhang, G., 2020. Emerging and legacy per- and polyfluoroalkyl substances in water, sediment, and air of the Bohai Sea and its surrounding rivers. Environmental Pollution 263, 114391. https://doi.org/10.1016/j.envpol.2020.114391

79. Zhou, Z., Liang, Y., Shi, Y., Xu, L., Cai, Y., 2013. Occurrence and Transport of Perfluoroalkyl Acids (PFAAs), Including Short-Chain PFAAs in Tangxun Lake, China. Environ. Sci. Technol. 47, 9249–9257. https://doi.org/10.1021/es402120y

Supplementary Materials

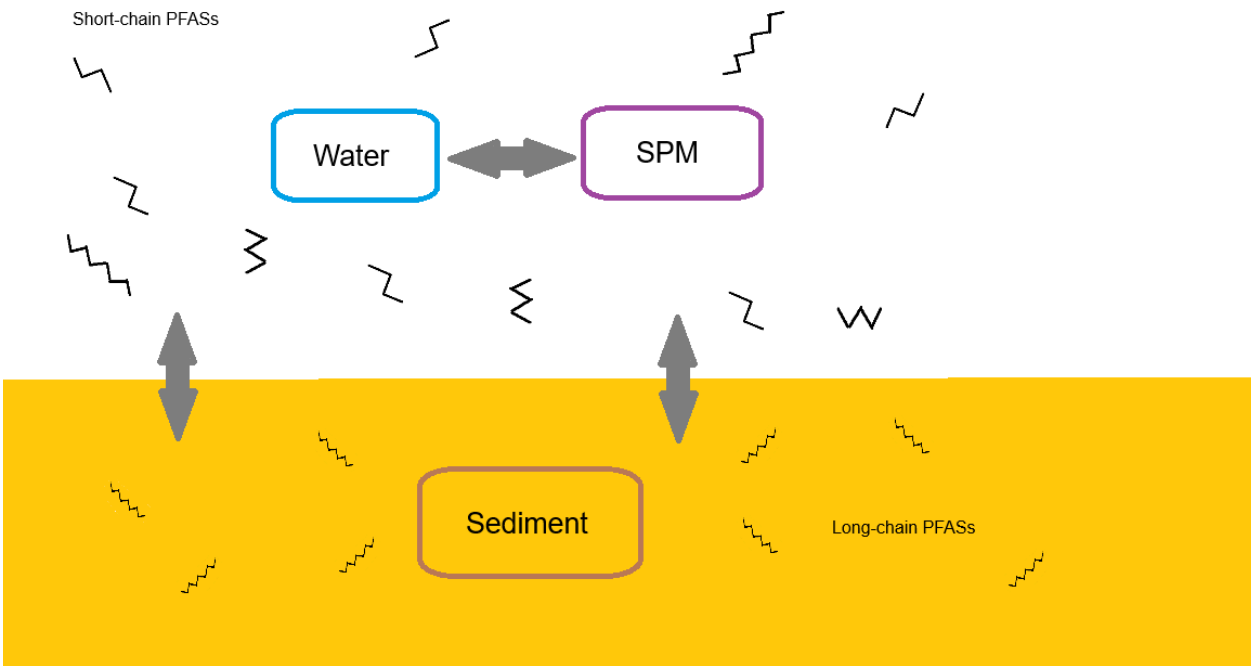

Figure S1. Visual Representation of long and short-chain PFAS in Water. SPM is suspended particulate matter. The image shows how short-chain PFASs are more prevalent in water while long-chain PFASs are more prevalent in sediment. This increased accumulation in water is part of why short-chain PFAS are dangerous to humans, as humans can consume them via drinking water. (Zhao et al., 2016)

Table S1. Effect of Increasing Chain Length on PFAS Properties at 25°C (ITRC 2023)

Number of Carbons	4	5	6	7	8	9	10	11	12
PFAS Molecule	Short-chain PFCAs				Long-chain PFCAs				
	PFBA	PFPeA	PFHxA	PFHpA	PFOA	PFNA	PFDA	PFUnA	PFDoA
Water Solubility (mg/L)	447	120	30	6.6	1.7	0.18	2.1	0.5	0.07
Vapor Pressure (Pa)	251	151	120	38	4.2	1.3	0.23	0.1	0.09
Critical Micelle Concentration (mg/L)	1.50E+05	60502	24950	8535	3767	1806	438	159	57
Log K_{oc} (± St. Dev.) in Sediment	1.45 (±0.05)	2.54 (±0.51)	2.72 (±0.4)	2.62 (±0.21)	2.63 (±0.45)	2.9 (±0.1)	3.05 (±0.3)	4.2 (±0.5)	4.4 (±0.2)

Table S2. Concentrations of Short-Chain PFAS Chemicals in Water in ng/L. NF means that the data was not found. (Sun et al., 2016; Ladapo, 2019; Thompson et al., 2024; Zhao et al., 2020; Heydebreck et al., 2015; Zhao et al., 2016; So et. al, 2007; Möller et al., 2010; Bai and Son, 2021; Nakayama et al., 2007; Zhang et al., 2016; Zhou et al., 2013; Gebbink et al., 2017; Pan et al., 2018)

Location	Min [PFBS]	Max [PFBS]	Min [PFHxA]	Max [PFHxA]	Min [GenX]	Max [GenX]
Yellow River	0	6.67	8.04	47.3	0	3100
Pearl River	0.03	0.13	0.13	0.67	0	663
Rhine River watershed	0.22	153	0.03	17.4	0	86
Truckee River	2.3	11.4	3.2	59.6	0	0
Las Vegas Wash	0	44.7	1.3	187	0	0
Cape Fear drainage basin	0	9.41	0	23	55	4500
Rhode Island, New York	0.09	6.2	0.49	48.4	0	15.3
Tangxun Lake	2240	4520	27.8	462	NF	NF
Merwede, Netherlands	0.54	27	0.1	6.4	0.2	812
Upper Mississippi River Basin	0	84.1	0	53.4	NF	NF